Engineering Structures 340 (2025) 120592

Contents lists available at ScienceDirect

Engineering Structures

journal homepage: www.elsevier.com/locate/engstruct

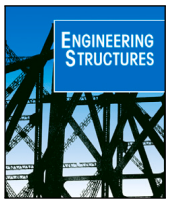

Fire resistance of wooden dowelled cross-laminated timber panels under in-plane loading

Angelo Aloisio [a,*,1], Dag Pasquale Pasca [b,1], Massimo Fragiacomo [a,1]

[a] Department of Civil, Construction-Architectural and Environmental Engineering , Università degli Studi dell'Aquila, L'Aquila, Italy
[b] Norsk Treteknisk Institutt (Norwegian Institute of Wood Technology), Oslo, Norway

ARTICLE INFO

Keywords:
Fire performance
Wooden dowels
Cross-laminated timber
Adhesive-free
Sustainability

ABSTRACT

This paper addresses the fire resistance of adhesive-free Cross-Laminated Timber (CLT) panels assembled with beech wooden dowels. A 180 mm thick, unprotected sample composed of six layers, each 30 mm thick, with overall dimensions of 3 m×3 m, was subjected to a standard fire curve for 100 min. The panel was loaded in-plane with a uniformly distributed load of 50 kN/m^2. During the large-scale fire test, the temperature on the unexposed side and deformations at various points were monitored. Additionally, the final reduction in cross-section along the panel's height was assessed. The overall fire performance of the wooden dowel CLT (WDCLT) panels was satisfactory, with no failure after 100 min of exposure. A thermomechanical analysis of the panel was conducted to simulate the panel's mechanical behaviour under fire. Since no temperature data within the panel or direct measurements of the evolving charring depth were available, validation was performed against the deformation history. The charring rate time history was indirectly estimated from the model. A parametric analysis was conducted to simulate the load-carrying capacity ratio over time for the WDCLT panels, considering multiple layups with 5, 6, and 7 layers, with respective thicknesses of 150 mm, 180 mm, and 210 mm. The performance of these WDCLT panels was also compared to that of models representative of glued CLT panels, discussing the sensitivity of the fire resistance to the charred layer fall-off.

1. Introduction

Over the past 20 years, CLT has established itself as an excellent construction material due to its good structural and non-structural properties [1–5]. Studies show that CLT construction results in lower greenhouse gas (GHG) emissions compared to conventional reinforced concrete, as demonstrated through life-cycle analysis (LCA) [6]. However, the environmental benefits of engineered wood products are compromised by the use of adhesives, which are essential for bonding the timber layers to create products such as LVL, GLT, and CLT. These adhesives not only reduce the sustainability and recyclability of the panels but may also pose health risks due to the release of harmful Volatile Organic Compounds (VOCs) and formaldehyde. Glue-laminated timber panels commonly rely on adhesives such as phenol-formaldehyde (PF) or polyurethane (PUR) for effective bonding [7,8]. Despite adhesives making up only 1.4% of the total panel mass, they account for nearly one-third of the product's environmental impact [9,10]. Since adhesives are derived from petroleum-based materials, their future availability is uncertain [11]. Lignin-based adhesives offer a promising alternative but only perform comparably to conventional systems when mixed with 50% phenol [11]. Additionally, some natural adhesives are solvent-based and require careful handling [12]. Adhesives also affect engineered wood products' end-of-life disposal, reusability, and recyclability [9].

In recent years, research has increasingly focused on developing engineered wood products without adhesives, instead using mechanical connectors such as beech dowels. While metal connectors are widely used and effective, wood-based connectors, such as wooden dowels or nails, are being explored as a more eco-friendly alternative [13,14]. These connectors are fully compatible with the wood material, improving disassembly and recyclability. Salvaged plywood tenons have been successfully used as connectors in dowel-laminated timber, increasing bending stiffness by 40% compared to unconnected members [15]. Numerical studies have shown that dowel diameter and spacing significantly impact the stiffness and load capacity of dowel-laminated timber members [16], while experimental studies confirm that larger dowel diameters and more dowels improve the flexural modulus of adhesive-free laminated timber and cross-laminated timber panels [17].

* Corresponding author.
E-mail addresses: angelo.aloisio1@univaq.it (A. Aloisio), dpa@treteknisk.no (D.P. Pasca), massimo.fragiacomo@univaq.it (M. Fragiacomo).
[1] All authors equally contributed to this reserach.

https://doi.org/10.1016/j.engstruct.2025.120592

Interestingly, dowel insertion angles and species have minimal impact on structural performance [17], though further research on optimizing dowel patterns, shapes, and numbers is necessary.

Typically, dowels are hydraulically inserted into pre-drilled holes, but high-speed rotational dowel welding has emerged as an innovative method. The friction from the dowel rotation generates heat, softening the lignin at the interface and creating a weld line upon cooling, which enhances the dowel's withdrawal strength and mechanical performance [10,18]. However, the durability of welded joints remains a concern, often requiring resins to achieve satisfactory results [19]. Studies have shown that dowelled beams with welded connectors outperform nailed beams, even when twice as many nails are used [20]. A novel process involving dowels soaked in sunflower oil before welding has shown efficiency, achieving stiffness relative to a fully composite system of 49% to 74% [20]. Most failures in these systems are due to dowel fractures, and hardwood fasteners in softwood layers may further enhance performance. Concerns over dowel shrinkage from reduced humidity can be addressed using densified wood dowels, prone to swelling and easing the manufacturing process [21]. Finally, standardized certification processes are necessary to bring dowel-laminated products to market [10].

Even though adhesive-free wood products have been studied for many years, the dominance of commercial adhesive-based products has slowed research in this area, even though there is a market demand for such products [9,22]. As a result, research on wooden dowel CLT has significantly lagged, leaving many aspects still unclear, particularly regarding the structural reliability of panels exposed to varying moisture content and temperatures and their fire resistance. This paper examines the fire resistance of wooden dowel CLT panels.

It is well known that massive timber elements perform well under fire conditions, as charred wood acts as an insulating barrier, reducing heat transmission to inner fibres. Extensive research has been conducted on the thermal and mechanical behaviour of glued CLT panels under fire, which differs from other wood-based products like glulam. This variation is influenced by factors such as raw material, adhesive type, panel thickness, number of layers, intended use (floor or wall) and the potential application of fire-resistant cladding materials. Studies, both small-scale [23–25], large-scale [26–30] and full-scale [31], have been carried out on CLT panels with various configurations and load conditions, indicating that fire behaviour is significantly impacted by the number and thickness of layers and the adhesive type used. In particular, temperature-sensitive adhesives can cause charred layers to fall off, especially in floor elements. However, the charring behaviour of CLT is unaffected by layer orientation (parallel or perpendicular) [32,33]. Charring rates for unprotected CLT specimens, without charred layer detachment, align well with values suggested by EN 1995-1-2 [34], although these rates can vary depending on the fire curve [26]. Recent studies have also explored the effects of fire retardants and coatings on the fire performance of engineering wood products [35,36].

However, to the authors' knowledge, no specific research has been dedicated to studying adhesive-free CLT panels, likely due to their niche market of such products and the high fire test costs, which can only be conducted at specialized institutions. In particular, the distinction between adhesive-based CLT and WDCLT under fire conditions is poorly documented. While it is well established that massive timber elements, including CLT, generally perform well in fire due to their predictable charring behaviour and insulating properties, adhesive failure in glued CLT can lead to delamination and premature loss of load-bearing capacity. In contrast, WDCLT, which relies on mechanical interlocking rather than chemical bonding, behave differently: wooden dowels can act as heat bridges, transferring thermal energy between layers, but they also eliminate the risk of adhesive degradation and related char fall-off. Moreover, due to the lower slip modulus among layers in WDCLT, the relative impact of losing one or more layers under fire exposure may be less critical compared to adhesive-bonded CLT, where delamination can cause a sudden and significant reduction in stiffness and capacity. Whether these characteristics translate into better or worse overall fire resistance remains an open question. This study addresses this gap by experimentally investigating the fire behaviour of full-scale WDCLT panels under standardized conditions.

The WDCLT panels considered in this work are obtained by joining timber layers using wooden dowels, arranged in a staggered pattern and inserted into pre-drilled holes after kiln drying. The dowels swell after insertion as they regain moisture, achieving equilibrium with the wood and the environment and ensuring mechanical integrity. However, the nature of this assembly could potentially pose challenges for fire resistance and mechanical stability. Differential shrinkage between the timber boards and the dowels may lead to loss of contact and the disassembly of the panel. This could occur because environmental conditions might restore the insertion state, eliminating friction between the dowels and the timber. In fire scenarios, this risk is amplified as the rapid drying of dowels could lead to loss of contact and layer separation. However, it is unclear if this issue is more severe than the loss of mechanical properties of adhesives under fire and the resulting delamination in glued CLT panels. Therefore, understanding the fire resistance of wooden dowel CLT, especially in comparison to traditional glued CLT, is crucial.

This study presents the experimental results from a large-scale fire test conducted on a nearly 3 m × 3 m WDCLT panel, 180 mm thick, with six layers under an in-plane distributed load of 50 kN/m^2 , following the DIN EN 1363-1 [37] standard. The buckling load of the WDCLT panel, estimated according to Eurocode 5, is approximately 210.60 kN/m, leading to a load ratio of 0.24. The panel was exposed to the standard fire curve on one side and 20 °C on the other. The fire resistance was evaluated, with temperatures monitored on the unexposed side, along with deformation data. These experimental results were used to validate a thermomechanical model developed in MATLAB, which was then employed to derive load-bearing capacity versus time curves for three WDCLT products from BIOHABITAT, with thicknesses of 150 mm, 180 mm, and 210 mm. These curves were compared with those of glued CLT. The parametric analysis aimed to estimate the dependence of fire resistance on the cross-section's geometric properties (depth and layout) and the applied load level.

2. Wooden dowelled cross-laminated timber panels

The wooden dowel CLT (WDCLT) wall, produced by BIOHABITAT, is a solid mass timber panel of 150 mm wide and 30 mm thick timber boards arranged in vertical, horizontal, and diagonal orientations. The layers are mechanically bonded by pressing beech dowels, 16 mm in diameter, into place under approximately 30 atm of pressure. The production process begins with the fabrication of the dowels. The 16 mm dowels are shaped using a lathe, cut to the required length, and oven-dried for at least 48 h. This drying process reduces their moisture content and causes a slight shrinkage in diameter. The boards are air-dried naturally and then kiln-dried until their internal moisture content is no higher than 10%.

Once the dowels are ready, the panel layers are assembled. The edges of the panels are compressed using hydraulic jacks to tightly press the lamellae together, minimizing any gaps between them. A uniform load is applied to the top surface to prevent the boards from lifting during assembly. Holes are pre-drilled with a 10 mm bit, followed by final drilling before the insertion of 16 mm diameter beech dowels under pressure of up to 30 atm. After inserting the beech dowels under pressure of up to 30 atm, they are sprayed with water to swell and ensure a tight fit. They are then stabilized along with the boards at a moisture level of around 12%. Finally, the completed panels are left to air dry for about a month, allowing the moisture content of the lamellae and dowels to equalize. At the time of assembly, the MC of the beech dowels was approximately 8%, while the Norwegian spruce boards had a moisture content of about 12% (see Fig. 1).

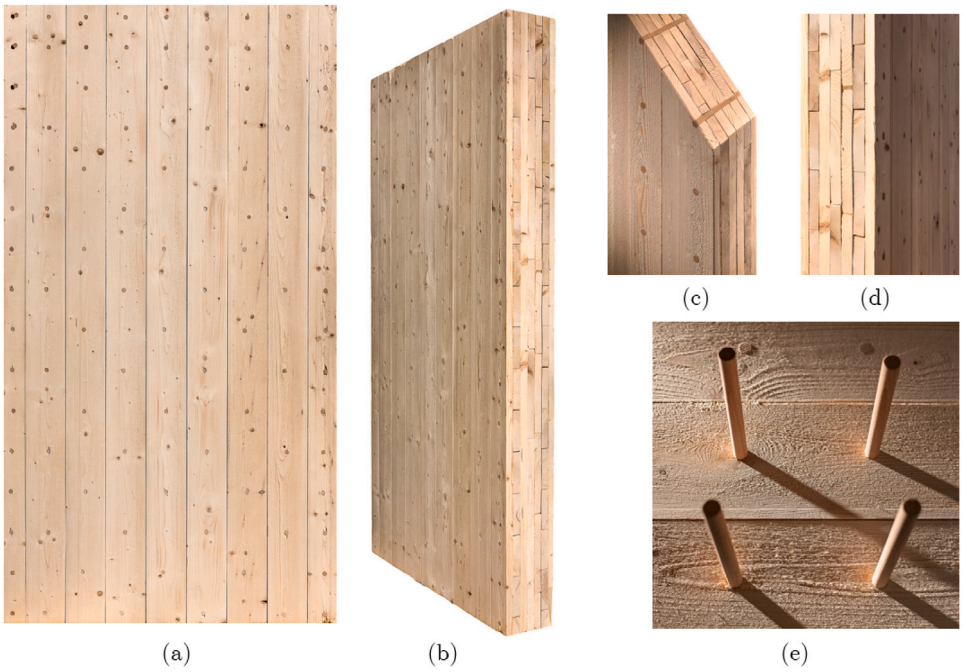

Fig. 1. Views of the wooden dowel CLT panels and details of the structural element. (a) front view, (b) lateral view, (c) cross-section with dowel, (d) cross-section without dowel, (e) Dowel in position before insertion.

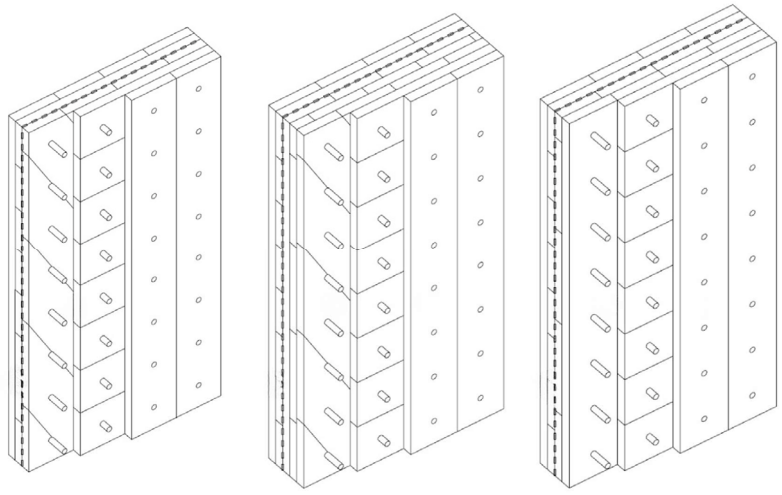

Thickness [mm]:	150	180	210
No. of Layers:	5	6	7
Layup:	(P-O-D1-O-P)	(P-O-P-D1-O-P)	(P-O-P-D1-D2-O-P)

P=parallel; D1= diagonal 30°; D2=diagonal 150°; O=orthogonal

Fig. 2. Layups of the Wooden Dowel CLT panels produced by the BIOHABITAT company.

The wall can be produced in various thicknesses, ranging from 150 mm to 270 mm, as shown in Fig. 2. The most commonly used thicknesses are 180 mm and 210 mm, with 150 mm typically used for internal load-bearing walls. The complete layer composition for these thicknesses is symbolically represented in Fig. 2, with the outer layers always oriented vertically.

The dowel layout, including spacing, edge, and end distances, follows the patented manufacturing system developed by BIOHABITAT srl, the producer of the WDCLT panels. In this configuration, dowels are placed at 150 mm spacing around the perimeter (at every board intersection), and at 300 mm spacing in the central portion, as shown in Fig. 2.

In this study, the authors analysed the fire performance of the 6-layer panels (180 mm thick).

3. Large-scale fire test

3.1. Specimen and test description

The tested wall was 180 mm thick (see Fig. 2) and acted as both a support and an enclosure for the furnace. Its overall dimensions were 2980 mm × 3000 mm. No electrical components, such as outlets or switches, were installed. The wall specimen was mounted within a test frame without additional fastenings. It was secured by applying

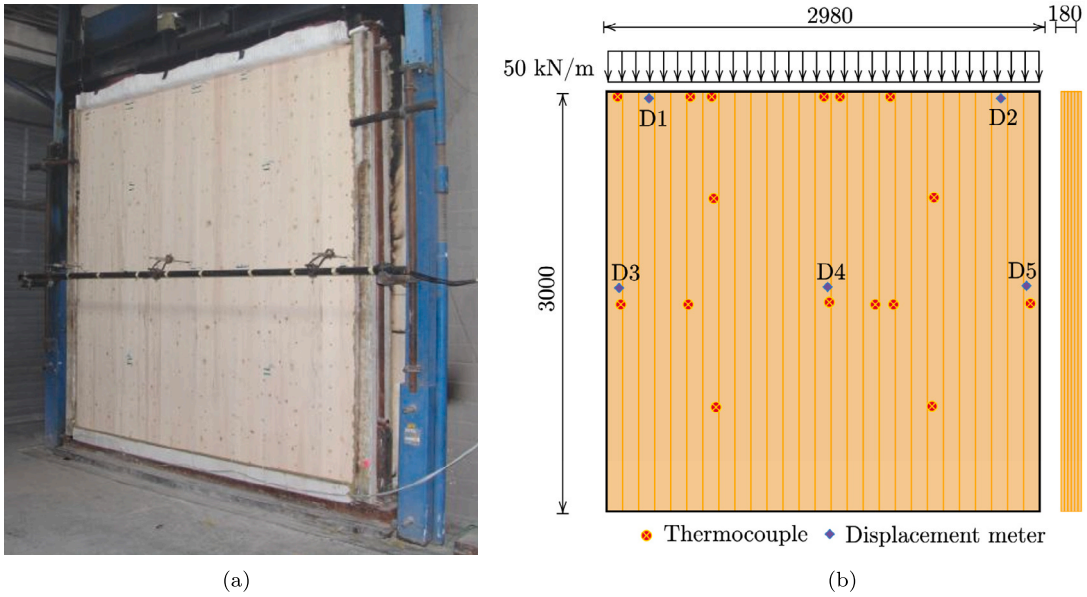

Fig. 3. (a) View of the unexposed side of the WDCLT panel before the fire tests; (b) experimental setup.

Table 1
Observations during the fire resistance test where F and FA stand for fireside and far fireside, respectively.

Test time [min:s]	Observations during the test	Observation side
−30:00	Application of load over 15 min.	–
−15:00	Load (50.0 kN/m) applied completely.	–
1:00	Beginning discolouration of the wood surface.	F
2:00	Blackening of the wood surface.	F
5:00	Beginning carbonization of the wood surface.	F
7:00	Vertical joints of the wood segment widen due to combustion.	F
13:00	Increasing carbonization of the wood and vertical joints continue to open.	F
19:00	Vertical joints continue to open, opening dimension 7 mm.	F
43:00	Minor smoke leakage from the first joint of the wood segment in the top area.	FA
48:00	A low crackling noise was heard in the specimen.	–
51:00	Noise in the furnace, probably wood components dropped into the furnace space.	–
63:00	Louder crackling noise in the specimen.	–
80:00	A crackling noise was heard in the specimen.	–
90:00	Minor smoke leakage from the first joint of the wood segment in the top area continues.	FA
100:00	End of fire test.	–

a continuous load of 50.0 kN/m to the structure. The vertical load was applied by two jacks and was distributed by a transverse beam. The boundary condition at the panel soffit can be idealized as semi-rigid, approaching a clamped condition due to the transverse beam restraining rotation. However, for conservative estimation, a hinged–hinged support configuration can be assumed. The fire exposure followed the standard temperature/time curve (ETK) per DIN EN 1363-1 [37]. The objective of the fire test was to evaluate whether the panel could maintain structural integrity under a sustained distributed load for 100 min of fire exposure. The vertical gaps between the wall and the test frame were filled with non-combustible mineral wool with a melting point above 1000 °C. The panel's initial moisture content was 6.50%, while the beech dowels' was 6.28%. Specialists from MFPA Leipzig carried out the fire tests.

Six plate thermometers were positioned 100 mm from the wall to measure temperatures within the fire space, which controlled the temperature within the fire environment. Additionally, sixteen NiCr-Ni thermocouples were installed on the unexposed side, as shown in Fig. 3. All surface temperatures were recorded at 10-s intervals. The ambient temperature was measured laterally, 1 m away from the specimen, at the same height as the test specimen. The pressure inside the fire space was also monitored per DIN EN 1363-1 using a differential pressure transmitter. The in-plane and out-of-plane displacement of the panel was monitored using potentiometric distance sensors, as shown in Fig. 3.

3.2. Main observations and fire resistance

Before discussing the results, it is essential to note that the experimental data from the thermocouples installed on the unexposed surface showed that the temperature remained constant throughout the tests, with a slight increase up to around 40 °C in the final stages, as shown in Fig. 4(a). Additionally, the temperature in the furnace closely followed the ISO standard temperature–time curve, as shown in Fig. 4. Fig. 4(b) also displays the variation in pressure inside the furnace, which did not exceed an average of 20 Pa.

Table 1 presents the main phases of the test up to 100 min. Specifically, Fig. 5 shows four phases of the fire test. (a) After three minutes, the panel had completely blackened the exposed surface, while (b) shows the panel after eight minutes. (c) and (d) display the final stages when the panel is removed from the furnace. No panel failure occurred at the end of the 100 min. Based on the test results, the in-plane loaded WDCLT panel achieved a fire resistance period of at least 100 min during one-sided fire exposure.

Fig. 6 provides a detailed view of the panel after the fire was extinguished, highlighting the areas where the charred layer remained. The first two charred layers, both vertical and horizontal, fell. The 3rd was also entirely charred, and the 4th only partially, but these two did not fall. In particular, Fig. 6(b) shows the parallel and diagonal layers. Direct inspection of the panel after the test did not reveal any

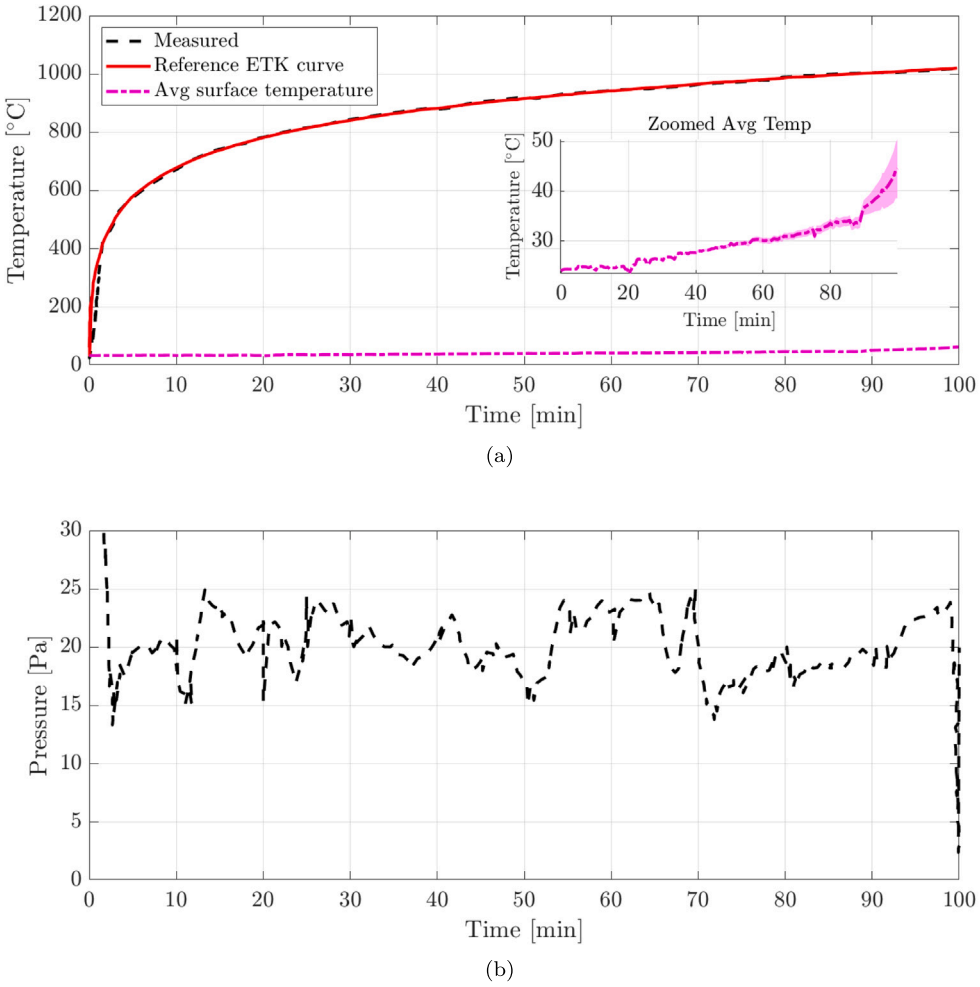

Fig. 4. (a) Temperature–time curve in the furnace compared to the ISO curve with average surface temperature on the unexposed surface in the inner plot (b) Pressure–time curve measured in the furnace.

Table 2
Summary of test results.

Load (kN/m)	Cladding	Ambient Temp. (°C)	Duration (min)	Failure	Residual section (mm)	Avg charring rate (mm/min)
50	No	20	100	No	104	0.9

substantial difference in charring depth between the central zones of the timber and the interface areas with the dowels. It is also noted that there was no clearance between the dowels and the timber boards at the time of testing, due to the swelling of the dowels. This swelling occurs as a result of the moisture content difference between the dowels and the surrounding timber at the time of insertion, as explained in Section 2. The residual cross-section was measured at 16 different locations along the midline of the specimen, as shown in Fig. 7, confirming the detachment of the first two layers. Thus, the equation below expresses the average residual cross-section along the midline.

$$h(x) = \begin{cases} 76 & \text{if } 200 \le x \le 2800 \\ 130 & \text{otherwise} \end{cases} \quad (1)$$

Table 2 summarizes the test results and provides an average estimate of the charring rate, calculated by dividing the final charred depth by the test duration. The average charring rate was approximately 0.9 mm/min, slightly higher than that of glued CLT, GLT panels, and solid timber [38], with variability along the height (see [39,40] showing a charring rate equal to approximately 0.8 for unprotected vertical CLT panels). It ranged from around 0.4–0.5 mm/min at the edges to just over 1 mm/min in the central area of the panel.

Since temperature measurements within the panel's section and direct measurements of the charred depth at intermediate intervals were not available, the progression of the charring rate over time was indirectly estimated from the continuous deformation measurements, shown in Fig. 8. This was done by solving an optimization problem using the panel's thermomechanical model, as explained in the following section.

The displacement time-histories, shown in Fig. 8, indicate a nonlinear increase in displacement both in-plane (measured at two points at the top of the panel, D1 and D2) and out-of-plane (estimated at three points along the midsection). In the curve in Fig. 8(a), there is a segment just before 40 min characterized by a rapid increase in deformation. The step-like behaviour in both load capacity and deformation is typical of CLT. This is because charring of the weaker layer (where the grain is perpendicular to the load direction) does not significantly reduce strength. In contrast, charring of the longitudinal layer (with the grain parallel to the load direction) can lead to a considerable decrease in strength and an increase in deformability. Interestingly, during this test, one parallel layer, one perpendicular layer, and another parallel layer were progressively consumed, with partial charring of a diagonal layer. Without a detailed model, it is difficult to determine the exact scenario when the deformation rise occurred.

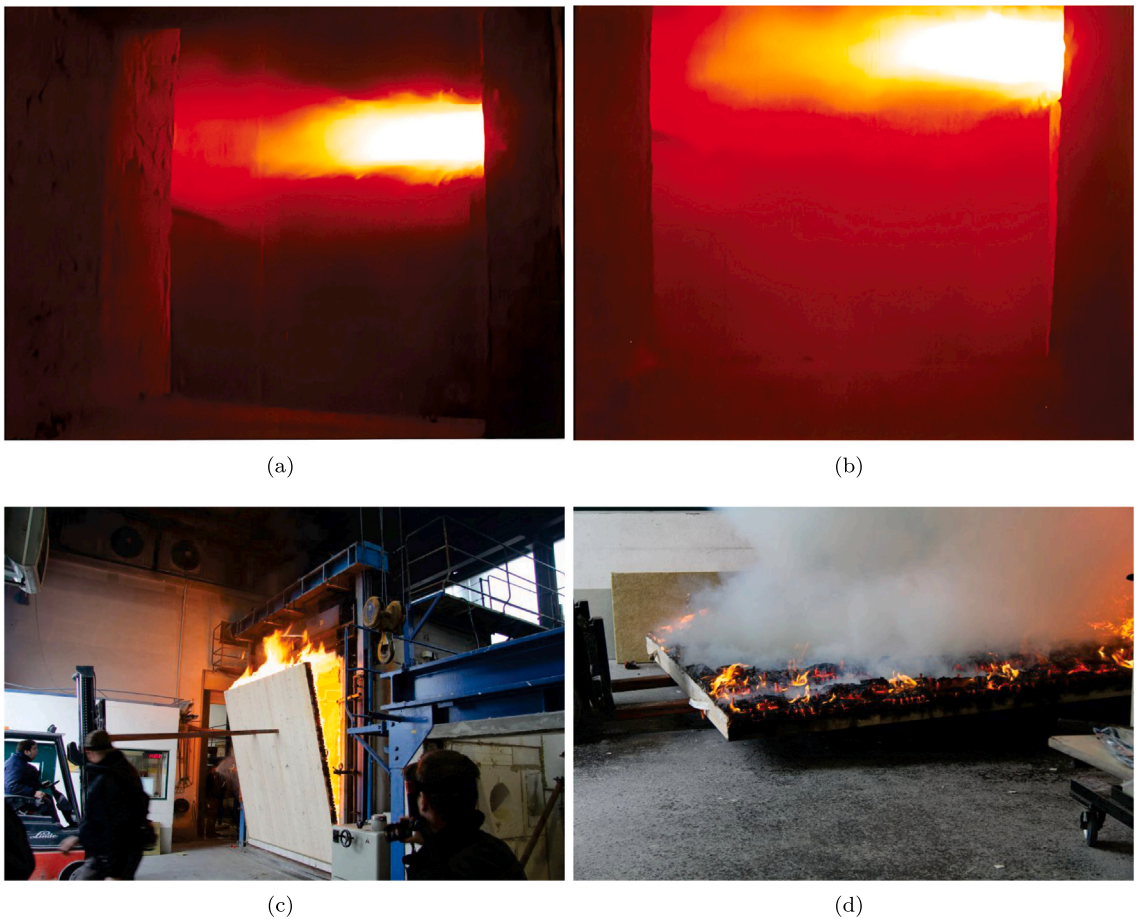

Fig. 5. (a) Minute 3: Surface fully blackened, (b) Minute 8, (c)–(d) Panel after the test.

Fig. 6. (a)–(b) View of the panel after the test.

The out-of-plane behaviour is more challenging to interpret, as the central sensor even shows a change in displacement direction. This is due to the combination of increasing out-of-plane deformation caused by the reduced cross-section under constant load and thermal deformations of the panel, leading to possible opposite displacements in the central area and at the edges. The displacement histories recorded during the fire test allowed the authors to calibrate the thermomechanical model to predict the charring rate throughout the test and then perform parametric analyses using the calibrated model.

In conclusion, the tested wall structure met the criteria for load-bearing capacity, space enclosure, and heat insulation specified by DIN EN 13 501-2: 2010-02, achieving fire resistance class REI 90 under one-sided fire exposure. First, the wall's load-bearing capacity was maintained, with an initial maximum load of 50.0 kN/m applied. Regarding vertical compression deformation, the limit value of 30 mm was not reached. The rate of change in compression strain also fell within the limits. No fissures were detected, as confirmed by the fact that a feeler gauge could not penetrate through cracks. Furthermore, no flames developed on the unexposed side of the wall during continuous fire exposure. For heat insulation, the maximum temperature increase on the unexposed side of the wall remained within the allowable range. Specifically, the maximum allowable mean temperature increase of 140 K and individual value of 180 K was not exceeded at any point.

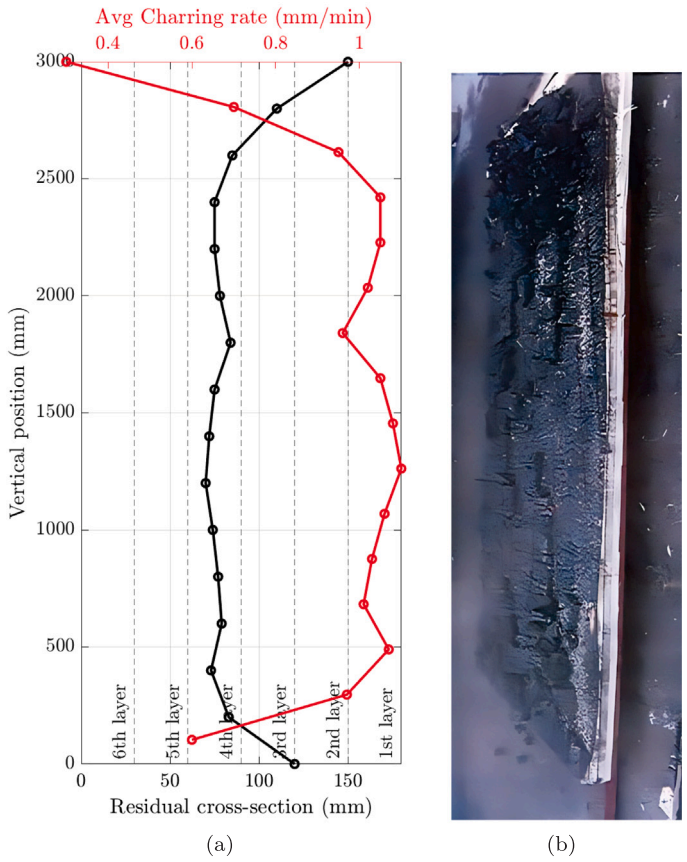

Fig. 7. (a) Residual cross-section and average charring rate after the test; (b) panel after the test.

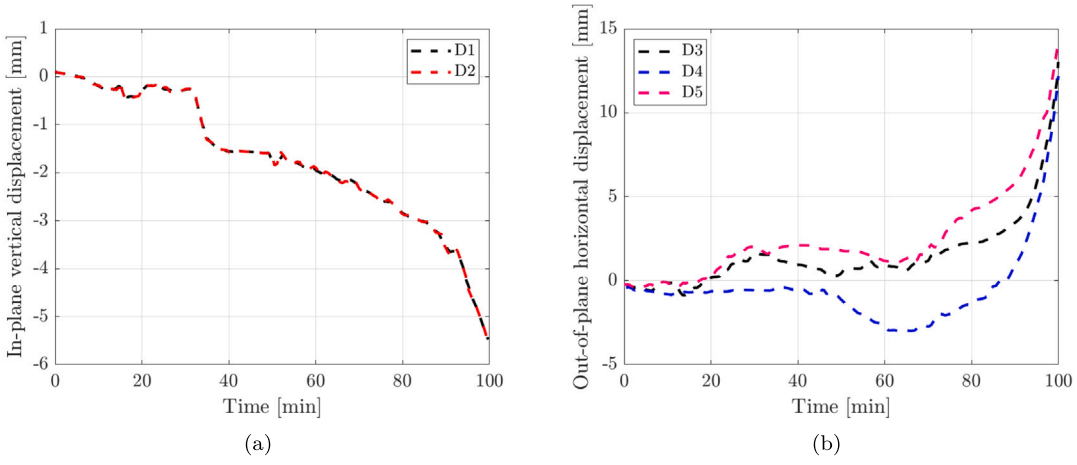

Fig. 8. (a) in-plane and (b) out-of-plane displacement of the panel in the positions marked in Fig. 3(b).

Additionally, the ambient temperature at the beginning of the test was recorded at 17 °C, with a maximum increase of 3 K during the test.

3.3. Single burning tests

The classification system for the fire reaction properties of building materials in Europe was introduced over two decades ago [41]. Known as the Euroclass system, it provides a standardized framework for assessing the fire performance of construction products. The system includes two primary categories: one for construction materials excluding floorings (mainly wall and ceiling linings) and another for floorings. Both categories are graded from A to F, with classes A1 and A2 representing non-combustible products. This system is detailed in Table 3 and has been fundamental for harmonizing fire safety standards across Europe [42].

In this investigation, an SBI (Single Burning Item) test was carried out, as shown in Fig. 9, following the EN 13823 [43]. The goal is to evaluate the reaction to fire of the WDCLT when exposed to a thermal attack from a single burning item. The test assesses how the material behaves under fire conditions, particularly its contribution to spreading fire and releasing heat and smoke.

Fig. 10 plots the time-histories of the FIGRA (Fire Growth Rate), HRR (heat release rate), THR (Total Heat Release), SPR (Smoke Production Rate), SMOGRA (Smoke Growth Rate) and TSP (Total Smoke

(a) (b)

Fig. 9. WDCLT panel (a) before and (b) after the Single Burning Test.

Table 3
Overview of the European reaction to fire classes for building products excluding floorings.

Euroclass	Smoke class	Burning droplets class	Non-comb	SBI Small flame	FIGRA W/s
A1	–	–	x	–	–
A2	s1, s2 or s3	d0, d1 or d2	x	x	≤120
B	s1, s2 or s3	d0, d1 or d2	–	x	≤120
C	s1, s2 or s3	d0, d1 or d2	–	x	≤250
D	s1, s2 or s3	d0, d1 or d2	–	x	≤750
E	–	d2	–	x	–
F	–	–	–	–	–

SBI = Single Burning Item [43], the main test for the reaction to fire classes for building products; FIGRA = FIre Growth RAte, the main fire class parameter according to the SBI test.

Table 4
Fire performance parameters for WDCLT. The table reports the Fire Growth Rate (FIGRA) at energy levels 0.2 MJ and 0.4 MJ, Total Heat Release after 600 s (THR600), Smoke Growth Rate (SMOGRA), and Total Smoke Production after 600 s (TSP600) for the tested panel.

Parameter	Unit	Test No. 1	Test No. 2	Test No. 3	Mean	CoV
FIGRA0.2 MJ	[W/s]	344	403	460	402	0.14
FIGRA0.4 MJ	[W/s]	344	403	460	402	0.14
THR600	[MJ]	15	15	15	15	/
SMOGRA	[m^2/s^2]	2.3	2.1	2.1	2.2	0.05
TSP600	[m^2]	43	41	44	43	0.04

Production). The HRR curve for WDCLT shows an initial rapid combustion phase similar to that observed in glued CLT. The fire growth rate (FIGRA) shows a high peak early in the test. Still, it stabilizes, indicating a gradual fire spread. Additionally, the THR (Total Heat Release) curve for WDCLT shows a steady increase without jumps later in the test. This suggests that the wood burns consistently without the sudden exposure of uncharged material. The SPR (Smoke Production Rate) curve for WDCLT also shows a gradual increase before stabilizing, with no sign of adhesive layers contributing to excessive smoke. SMOGRA (Smoke Growth Rate) follows a similar pattern, with an early peak but quickly stabilizing.

Table 4 reports the main fire performance parameters for the tested panel: the FIGRA at energy levels 0.2 MJ and 0.4 MJ, THR after 600 s (THR600), SMOGRA, and TSP after 600 s (TSP600) for the tested panel. Based on the results obtained in Fig. 10 and Table 4, the WDCLT has been classified as D-s1, d0; see Table 3. In the case of glued CLT, the classification is often around D-s2, d0, as it produces more smoke (TSP > 50 m^2), but generally does not produce flaming droplets [44,45]. Glued CLT typically generates higher smoke levels due to the burning of adhesives, which can release VOCs and other harmful substances during combustion. Based on this test, WDCLT tends to have a slightly better classification than glued CLT due to lower smoke production [44,45]. Therefore, it can be concluded that the fire performance of glued and non-glued vertical unprotected CLT panels is quite similar. Although the charring rate appears slightly higher for WDCLT, the smoke class is better. A classification of D-s2, d0 or D-s1, d0 is typical for many bio-based structural and non-structural materials such as plywood and OSB [42]. It is also important to note that no tests were conducted with horizontal panel orientation, where delamination in glued CLT panels typically occurs. This might reveal more significant differences in performance compared to WDCLT, but it is beyond the scope of this study.

4. Numerical model

4.1. Methods

A thermomechanical model was used to analyse the fire behaviour of vertical and unprotected WDCLT exposed to fire on one side. Specifically, heat transfer and mechanical analyses were conducted sequentially to simulate the thermal and structural responses of the WDCLT, respectively.

4.1.1. Thermal model

Wood's thermal and mechanical properties vary with temperature, following the relationships outlined in EN 1995-1-2 [34], which were implemented in MATLAB (see Fig. 11). The first step is to estimate the temperature evolution across the panel thickness, which is then used to determine the mechanical parameters.

The temperature distribution inside the WDCLT panel was obtained using a one-dimensional diffusion model with a variable thermal conductivity coefficient. The heat equation was solved under boundary

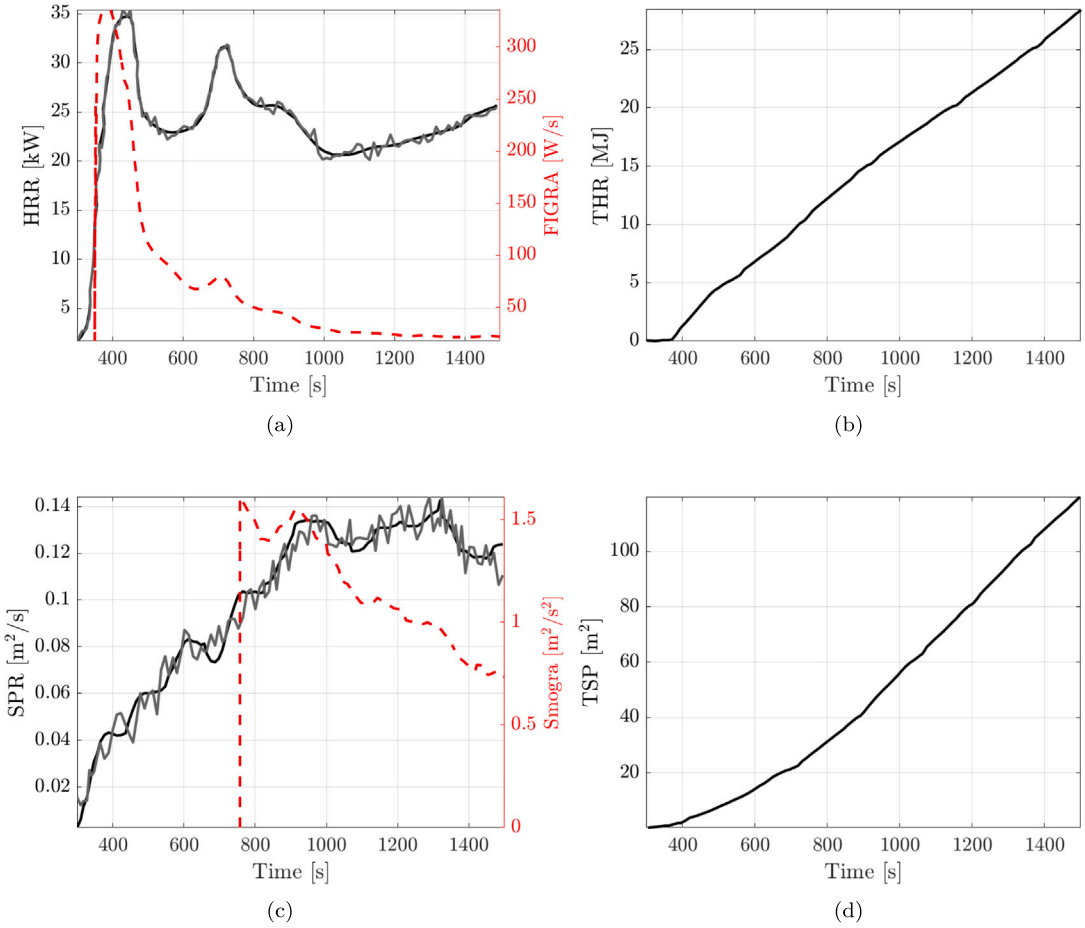

Fig. 10. (a) Time-histories of the FIGRA (Fire Growth Rate) and HRR (heat release rate). (b) Time history of the THR (Totalò Heat Release). (c) Time history of the SPR (Smoke Production Rate) and the SMOGRA (Smoke Growth Rate). (d) Time-history of the Total Smoke Production.

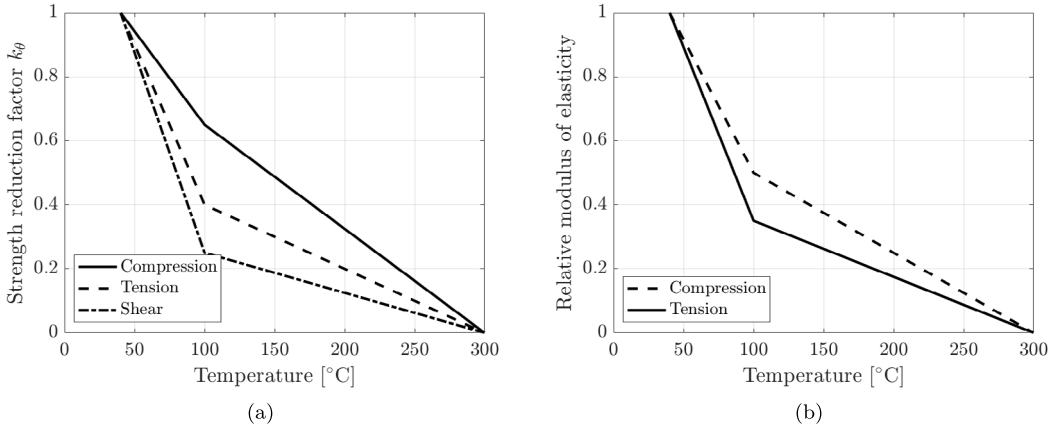

Fig. 11. (a) Strength and (b) modulus of elasticity reductions with temperature as suggested by EC5 (CEN 2004).

conditions, including convection and radiation. A temperature of 20 °C was applied on the unexposed side, while the furnace temperature was applied on the exposed side.

The governing monodimensional heat equation is:

$$\frac{\partial}{\partial x}\left(k(T)\frac{\partial T}{\partial x}\right) = \rho c \frac{\partial T}{\partial t}, \tag{2}$$

where $k(T)$ is the temperature-dependent thermal conductivity, $\rho = 450\,\mathrm{kg/m^3}$ is the density, $c = 1600\,\mathrm{J/(kg\ K)}$ is the specific heat capacity.

The boundary conditions are defined as follows. On the unexposed side:

$$-k(T)\frac{\partial T}{\partial x}\bigg|_{x=0} = h\left(T - T_\infty\right) + \epsilon\sigma\left(T^4 - T_\infty^4\right), \tag{3}$$

where $h = 25\,\mathrm{W/m^2\ K}$ is the convection coefficient, $\epsilon = 0.8$ is the emissivity, as recommended by EN 1991-1-2 [46] and EN 1995-1-2 [34], $\sigma = 5.67 \times 10^{-8}\,\mathrm{W/m^2\ K^4}$ is the Stefan–Boltzmann constant, T_∞ is the ambient air temperature set equal to 20 °C. On the furnace side:

Table 5
Temperature–thermal conductivity relationship for wood and the char layer.

Temperature (°C)	Thermal Conductivity (W m^{-1} K^{-1})
20	0.12
200	0.15
350	0.07
500	0.09
800	0.35
1200	1.50

Table 6
Framework for the capacity prediction of compressed timber elements according to Eurocode 5.

Framework for the buckling analysis of compressed timber elements

$$N_{c,0,Rd} = k_c N_{pl} \tag{5}$$

$$k_c = \begin{cases} 1, & \bar{\lambda} \le 0.3 \\ \frac{1}{k+\sqrt{k^2-\bar{\lambda}^2}}, & \bar{\lambda} > 0.3 \end{cases} \tag{6}$$

$$k = 0.5\left[1 + \beta_c\left(\bar{\lambda} - 0.3\right) + \bar{\lambda}^2\right] \tag{7}$$

$$\beta_c = \begin{cases} 0.2, & \text{Solid timber} \\ 0.1, & \text{Glued Laminated Timber} \end{cases} \tag{8}$$

$$\bar{\lambda} = \left(\frac{N_{pl}}{N_{ki}}\right)^{0.5} \tag{9}$$

$$N_{pl} = A_t f_{c,0,d,\mathrm{fi}} \tag{10}$$

$$N_{ki} = \pi^2 \frac{(EI)_{ef}}{(0.5L)^2} \tag{11}$$

$N_{c,0,Rd}$ is the buckling load, k_c the buckling reduction coefficient, k the buckling factor, $\bar{\lambda}$ the adimensional slenderness, β_c the imperfection factor, N_{pl} the plastic capacity of the timber element, N_{ki} the theoretical buckling load, A_t the cross-section area of the timber element, $f_{c,0,d,\mathrm{fi}}$ the design compression strength of timber parallel to the grain under fire load, $(EI)_{ef}$ the effective bending stiffness of the WDCLT panel, L the panel length.

$$T(x = H, t) = T_{\mathrm{furnace}}, \tag{4}$$

where T_{furnace} follows the ISO 834 fire curve [47] (see Fig. 4) and H is the panel thickness. The temperature–thermal conductivity relationship for wood and the char layer follows the values suggested by Eurocode (see Table 5).

The one-dimensional heat equation in Eq. (2) with variable temperature-dependent thermal conductivity was solved in MATLAB using the finite difference method.

4.1.2. Mechanical model

The mechanical model of the WDCLT panel is a one-dimensional beam with a layered cross-section. Each layer has different mechanical properties based on fibre orientation and the temperature distribution across the panel thickness.

The load-bearing capacity of the wall has been calculated following the Eurocode 5, which provides the method for the resistance for axially compressed timber elements [48,49]. Table 6 reports a set of equations for calculating the axial capacity of compressed timber elements.

The buckling coefficient in Eq. 8 is different than the one only for structural elements with relative slenderness higher than 0.3, where the slenderness in Eq. 9 is computed as the ratio between the plastic (Eq. 10 and the ideal buckling force (Eq. 11. The authors considered a clamped–clamped boundary condition and assumed an imperfection coefficient $\beta_c = 0.2$.

Table 7
Main mechanical parameters adopted in the analyses.

ρ [kg/m^3]	$E_{\parallel}$ [MPa]	$E_{\perp}$ [MPa]	E_{60} [MPa]	E_{120} [MPa]
450	11,000	367	1519	1519

The characteristic compressive strength of timber parallel to the grain ($f_{c,0,k}$) is assumed to be equal to 21 MPa. The design value in fire for compressive strength parallel to the grain ($f_{c,0,d,\mathrm{fi}}$) was calculated according to EN 1995-1-2 using the following formula:

$$f_{c,0,d,\mathrm{fi}} = k_{\mathrm{mod,fi}}\left(\frac{f_{c,0,20}}{\gamma_{\mathrm{M,fi}}}\right) = k_{\mathrm{mod,fi}}\left(\frac{k_{\mathrm{fi}} f_{c,0,k}}{\gamma_{\mathrm{M,fi}}}\right), \tag{12}$$

where $f_{c,0,20}$ and $f_{c,0,k}$ are, respectively, the 20th fractile and the characteristic value of compressive strength at normal temperature. The design value in fire was determined by assuming both the modification factor for fire $k_{\mathrm{mod,fi}}$ and the partial safety factor for timber in fire $\gamma_{\mathrm{M,fi}}$ equal to 1. The coefficient k_{fi} proposed by EN 1995-1-2 for glulam and wood-based panels was adopted with a value of 1.15. Substituting these values:

$$f_{c,0,d,\mathrm{fi}} = 1 \cdot \left(\frac{1.15 \cdot 21}{1.0}\right) = 24.15\,\mathrm{MPa}. \tag{13}$$

Thus, the design compressive strength parallel to the grain in fire is $f_{c,0,d,fi} = 24.15$ MPa.

The bending stiffness of the layered beam was estimated using the γ method, outlined in Appendix B of Eurocode 5, which provides a simplified approach to calculating the flexural characteristics of composite beams. The effective bending stiffness is computed using Eq. (14) [50]. This method is suitable when continuous fasteners maintain constant stiffness along the member's length, with negligible shear deformations over extended spans [51].

$$(EI)_{ef} = \sum_{i=1}^{3}\left(E_i \cdot I_i + \gamma_i \cdot E_i \cdot A_i \cdot a_i^2\right) \tag{14}$$

where E_i = Modulus of elasticity of the layers; I_i = Moments of inertia of the layers; A_i = Cross-sectional areas of the layers; a_i = Distance from the centroid of each layer to the neutral axis of the assembly. The gamma factor (γ_i) is computed using Eq. (15)

$$\gamma_i = \left(1 + \frac{\pi^2 \cdot E_i \cdot A_i \cdot s_i}{K_i \cdot l^2}\right)^{-1} \tag{15}$$

where s_i is the distance between connectors, K_i is the slip modulus of the connection and l panel span length.

It should be remarked that including the effect of mechanical fastening using wooden dowels is crucial since, for the same layup and material, using wooden dowels instead of glue can reduce bending stiffness by over 10 times. This significantly amplifies the P-δ effects, affecting the panel's load-bearing capacity.

The slip modulus, estimated using Eq. (A.1), is set equal to 1.69 kN/mm. Appendix details the push-out tests used for estimating the slip modulus. Such results are consistent with the stiffness of typical wooden dowel connections. For example, in [22], a value of 1.47 kN/mm is reported, which is very close to 1.69 kN/mm. Regarding the strength, the mechanical behaviour of wood was described as elastic-brittle in tension and elastoplastic in compression, considering the influence of the temperature according to Fig. 11.

The mechanical properties for the Elastic Moduli adopted in the analysis are provided in Table 7 and depend on the fibre orientation.

In particular, the transverse modulus is obtained from the following empirical formula, as reported in [52]:

$$E_{\perp} = \frac{E_{\parallel}}{30} \tag{16}$$

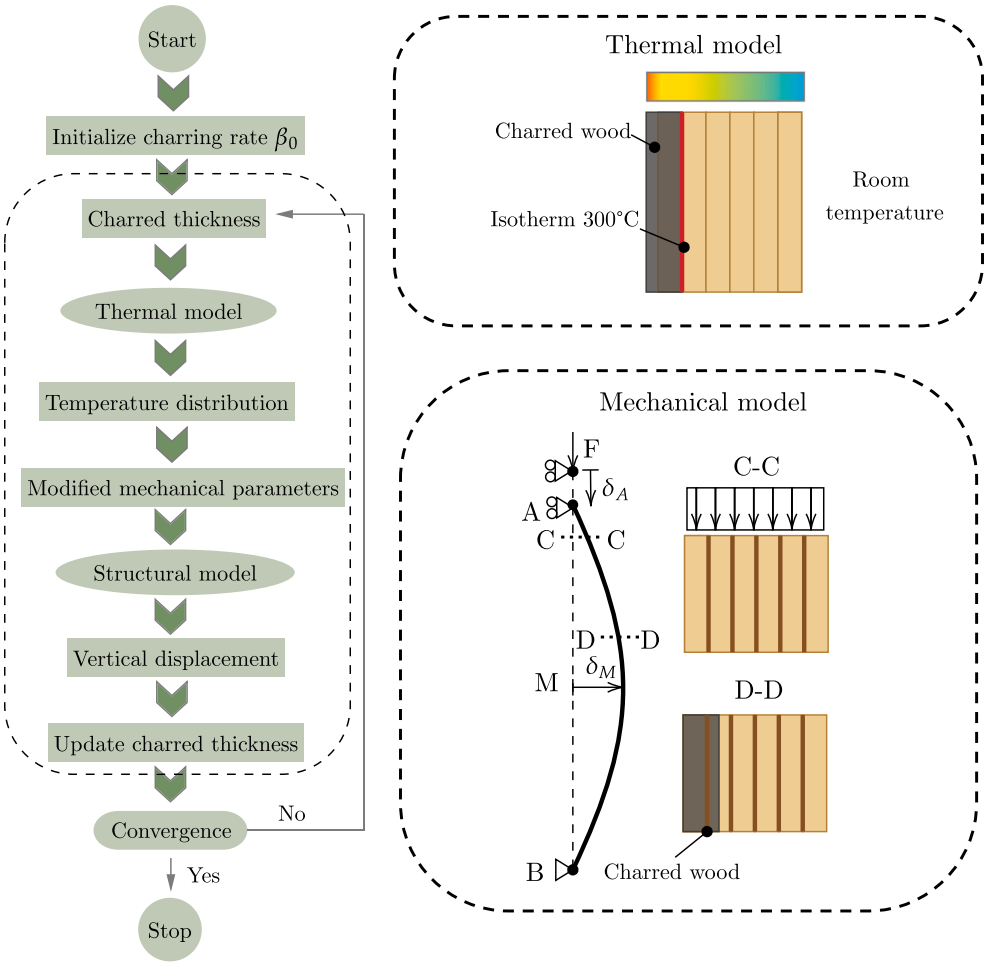

Fig. 12. Flowchart followed for assessing the time history of the charring rate from the performed fire test.

Meanwhile, Hankinson's formula [53] is used to estimate Young's modulus corresponding to a given angle of the fibres relative to the grain direction:

$$E_\theta = \frac{E_\parallel \cdot E_\perp}{E_\parallel \cdot \sin^2(\theta) + E_\perp \cdot \cos^2(\theta)} \tag{17}$$

where $E_\parallel$ is the modulus of elasticity parallel to the grain, $E_\perp$ is the modulus of elasticity perpendicular to the grain, and θ is the angle of the fibres relative to the grain direction.

The corrections to the mechanical parameters due to temperature are applied as follows. The beam section was divided into layers, each 1 mm thick, and each layer was assigned a reduction factor for the elastic modulus, used to calculate the effective bending stiffness ($(EI)_{ef}$) in Eq. (14), and a reduction factor for the compressive strength, used in Eq. 10

4.2. Indirect estimation of the charring rate

In the current paper, it was impossible to directly calibrate the thermal model as temperature values within the thickness were unavailable. However, since the vertical displacement history of the panel, shown in Fig. 8, is available, the mechanical model was used to indirectly estimate the time history of the charring depth, following the flowchart presented in Fig. 12.

After initializing with a given charring depth (d_{char}), a thermal analysis was first conducted to estimate the temperature distribution, followed by a mechanical analysis assuming the modified mechanical properties based on the temperature. The panel deflection was estimated under the uniformly distributed experimental load of 50 kN/m. Subsequently, the error between the estimated ($\delta_{\text{A,sim}}$) and experimental ($\delta_{\text{A,exp}}$) deflection was calculated. If the error exceeded 1%, the loop was repeated, updating the charring depth value.

$$\hat{d}_{\text{char}} = \arg\min_{d_{\text{char}}} \left| \delta_{\text{A,sim}} - \delta_{\text{A,exp}} \right| \tag{18}$$

At each iteration, convergence was reached step by step, allowing the time history of the charring depth to be estimated, which is crucial to understanding the progression of the fire behaviour.

At this stage, the temperature curve indicated by ISO 834 [47] was not used to estimate the 300 °C isotherm and assess the charred thickness. Instead, the charred thickness was assumed as an input parameter, and the thermal analysis was conducted by assigning a temperature of 300 °C at the charline and 20 °C on the unexposed surface.

It is important to note that the mechanical model, in addition to accounting for the modification of mechanical properties with temperature and the shear deformation of the panels due to the dowels, also includes the P-δ effect. It was observed that the charring rate near the load application was significantly reduced up to 20 cm from the edges; see Fig. 7. Therefore, the load distribution was always applied with the resultant force centred to the non-charred section of the panel, as shown in Fig. 12.

Fig. 13 shows the indirect estimation of the charring evolution results. Specifically, Fig. 13(a) shows the time evolution of the cumulative (right axis) and individual layer (left axis) uncharred thickness, while (b) that of the charring rate and the bending stiffness ratio.

The model, calibrated against the experimental results, leads to a final estimate of the charring depth close to 80 mm. After approximately 6, 30, and 90 min, the first three layers are entirely charred,

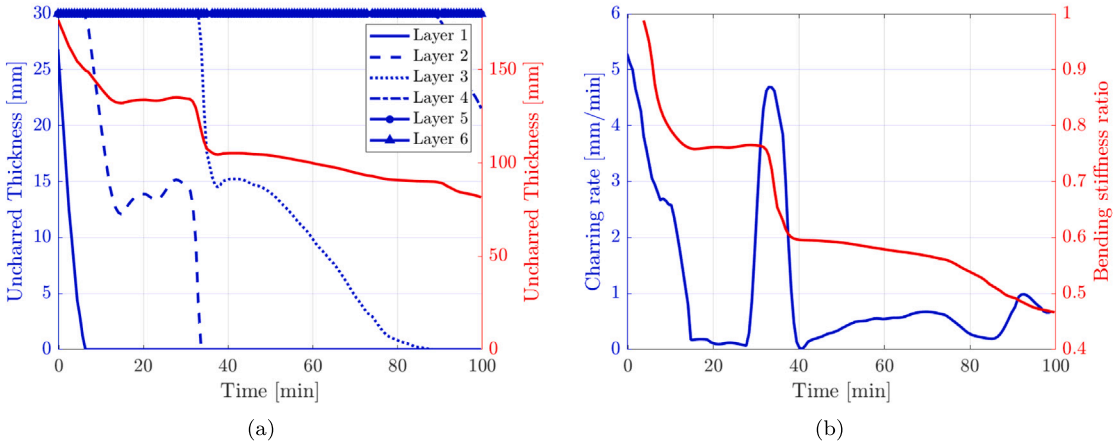

Fig. 13. (a) Time evolution of the cumulated (right axis) and single layer (left axis) uncharred thickness; (b) Time evolution of the charring rate and the bending stiffness ratio.

respectively. As observed in Fig. 6, the fourth layer remains only partially charred.

Since the curve is estimated from the deformation time history, it reflects the observed vertical deformation jump, occurring around 40 min. This jump corresponds to the charring of the third layer, which is parallel to the grain. It is plausible that, with the charring of the third layer, the increased panel deformation caused the charring layers of the first two layers to fall off, exposing the underlying wood surface. This led to a rapid increase in the charring rate up to 5 mm/min, which soon stabilized at values close to 0.5 mm/min. The evolution of the charring rate, estimated from the slope of the red curve, is also informative as it shows the non-stationarity of the charred layer, likely due to its detachment and inherent unevenness. As a result, the detachment of the first two layers (observed to have fallen off at the middle of the test as seen in Fig. 6) resulted in an average charring rate slightly higher than glued CLT wall panels. However, this remains consistent with tests on CLT, considering the difficulty in predicting the permanence of the charred layer and the inherent statistical uncertainty of such results. The charring curves show a plateau between 15 and 40 min, associated with the slowing of charring progression due to the insulating thickness of the charred layer, varying between 40 and 60 mm.

It should be remarked that, due to the absence of internal thermocouples, commonly used to track the temperature profile, the proposed indirect model calibration based on deflection data might introduce inherent uncertainty. Nonetheless, the estimated charring rates fall within the range reported in the literature for timber under standard fire exposure. For reference, Amin et al. (2024) [54] report an average charring rate of approximately 0.65 mm/min for CLT and glulam over 180 min of exposure, while other experimental studies have shown values ranging from 0.75 to 0.81 mm/min, with a mean of 0.79 mm/min—higher than those provided by EN 1995-1-2. Research on South African CLT [55] indicates average rates of 0.95 mm/min for SA pine and 0.76 mm/min for eucalyptus. For beech, a dense hardwood used in the present study alongside Norwegian spruce, typical charring rates range between 0.5 and 0.6 mm/min [56], depending on grain orientation and moisture content, which supports the observed values and trends in this work.

4.3. Parametric analyses

As highlighted in the introduction, parametric models are essential in fire engineering because fire tests are expensive and cannot account for all possible scenarios. In recent decades, numerical models have been increasingly employed to simulate the fire performance of wood-based materials, including laminated veneer lumber [57,58], GLT [59], and CLT [29,60,61]. However, large-scale fire simulations of WDCLT panels remain less unexplored.

In the parametric analyses, an uncoupled thermo-mechanical model was used to investigate the fire resistance of WDCLT panels. The study focused on three aspects: the effect of panel layups with 5, 6, and 7 layers (as shown in Fig. 2); a comparison between glued CLT and WDCLT panels; and the influence of charred layer detachment. The goal was to evaluate the load-bearing capacity evolution of three BIOHABITAT-produced panels, considering both perfect inter-layer adhesion, as in glued CLT products, and the slip modulus characteristic of the current inter-layer connection system. The thermal, mechanical, and geometric properties of the panels were assumed to be identical, as shown in Fig. 11.

Under the same loads, WDCLT panels exhibit greater vertical deformation than glued CLT due to dowel deformability. This increased deformation amplifies the P-delta effect and may reduce the load-bearing capacity. Furthermore, such deformation can lead to the detachment of the charred layer, exposing the uncharred wood and accelerating the charring process. Two scenarios were analysed: in the first, the charred layer detaches after two layers burn, limiting the charred thickness to 60 mm; in the second, the charred layer remains intact, providing continuous protection for the inner layers. Scientific literature supports analysing these limit cases [23,24]. In one case, the charred layer serves as insulation, reducing heat transmission into the panel. In the other, the charred layer delaminates, exposing inner layers directly to fire and accelerating heat penetration.

Initially, the authors assessed the impact of charred layer fall-off on the time-resistance curve of the tested panel, which consisted of six layers, each 30 mm thick. Fig. 14 illustrates the adimensional fire resistance of WDCLT walls, comparing (a) the scenario with delamination of the first two charred layers and (b) the scenario without delamination. It should be remarked that the term delamination will hereafter refer to the fall-off of the charred layer, even though, in principle, this phenomenon is attributed to glued laminated products.

As is typically observed, the load capacity curves of CLT exhibit distinct plateaus associated with the charring of layers where the grain direction is orthogonal to the applied load.

The authors included vertical lines to mark the completion of charring for each layer. Following the failure of the two layers, the delamination significantly accelerates the charring rate. The higher furnace temperatures further exacerbate this acceleration. In contrast, as shown in Fig. 14, the scenario without delamination gradually slows the charring process. Additionally, the authors simulated the case of two successive delaminations: one resulting in the collapse of the first two layers once consumed and another causing the collapse of the subsequent two layers.

Table 8 summarizes the time required to reach specific load ratio values, namely 70%, 50%, and 10% of the initial load. Most of the load-bearing capacity is eroded within the first 50 min. Consequently, the

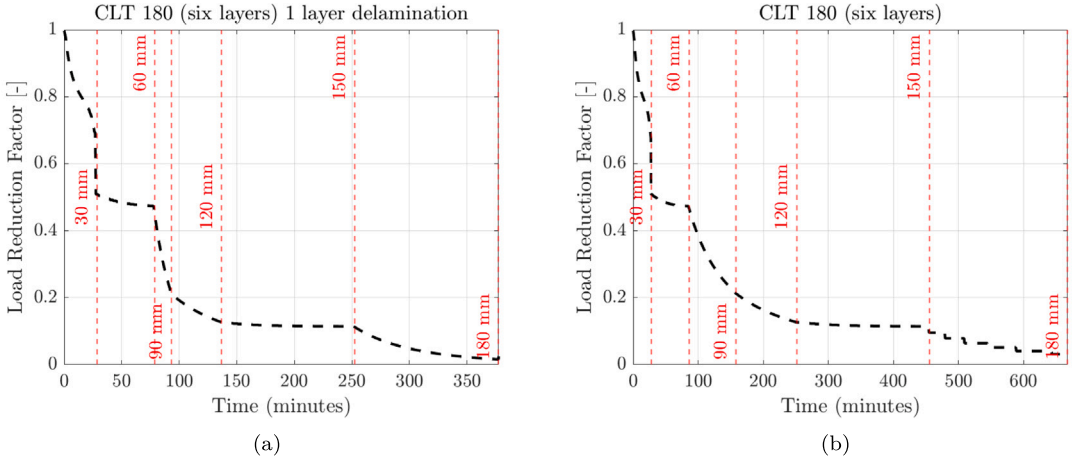

Fig. 14. Adimensional fire resistance of WDCLT walls (a) with and (b) without the delamination of the first two charred layers.

Table 8
Time values corresponding to the following load reduction factors, 70, 50, 10 and 1% with and without delamination of the first two charred layers of a six-layer WDCLT wall panel.

Specimen	No. Layers	Delamination	Time [min] at a given load ratio [%]		
			70%	50%	10%
WDCLT 180	6	1 layer	26	35	251
		2 layers	26	35	145
		No	26	35	454

Table 9
Time values corresponding to the following load reduction factors, 70, 50, 10 and 1% of five, six and seven layers 30 mm thick, glued CLT vs. WDCLT.

Specimen	No. Layers	Typology	Time [min] at a given load ratio [%]			
			70	50	10	0
CLT	5	Glue	9	17	80	140
		Wooden dowel	13	27	107	149
CLT	6	Glue	12	23	94	148
		Wooden dowel	26	35	145	179
CLT	7	Glue	17	43	123	159
		Wooden dowel	30	72	148	182

times associated with 0.7 and 0.5 load ratios are mainly unaffected by delamination, regardless of whether one or two delaminations occur. In contrast, the time corresponding to a 10% load ratio varies significantly among the three scenarios, ranging from 145 min with two delaminations, 251 min with one delamination, and nearly 450 min without delamination. Thus, delamination primarily affects the advanced stages of the curve, significantly impacting the time required to reach collapse.

In subsequent simulations, considering it more realistic that delaminations occur every two charred layers and recognizing that this assumption stands on the side of safety, the authors simulated the fire resistance over time of three panels with different layups: 5, 6, and 7 layers, see Fig. 2. Additionally, for each case, two scenarios were considered: (i) WDCLT with an inter-layer slip modulus of 1.69 kN/mm, as determined from push-out tests; (ii) Fully collaborating lamellae, as in the case of glued CLT.

Given the substantial differences in absolute performance between the two scenarios, owing to the superior mechanical properties of glued CLT compared to WDCLT, the fire resistance curves are presented in both adimensional and dimensional terms (as the load-bearing capacity per unit length).

Fig. 15 illustrates the adimensional fire resistance of WDCLT walls with delamination of the first two charred layers for panels consisting of (a)–(b) five, (c)–(d) six, and (e)–(f) seven layers, each 30 mm thick. Each subplot compares the performance of WDCLT against glued CLT.

First of all, Fig. 15(c) can be used to validate the parametric model. It shows that for the CLT180 case, half of the fourth layer is consumed approximately 100 min after the start of the test, as occurred in the large-scale fire test presented in this paper. This can be considered a validation of the parametric model, as it accurately predicts the progression rate of charring. Furthermore, at 100 min, the load-bearing capacity remains well above 100 kN/m, confirming that the model correctly predicts no failure under a load of 50 kN/m at 100 min from the start of the test.

As expected, the time needed to reach failure increases with the number of layers due to the additional material available to resist fire. Plateaus in the curves are associated with layers where the fibre orientation is orthogonal to the applied load. In contrast, layers with diagonal fibres exhibit intermediate slopes between the flat plateaus of orthogonal layers and the steeper slopes of layers parallel to the load. The simulation included two delaminations for the 5- and 6-layer panels, each occurring at the end of the charring process for a pair of layers. In the case of the 7-layer panel, three delaminations were simulated, with the final delamination occurring just before the last layer. Delamination significantly accelerates the charring process, particularly for internal layers, as furnace temperatures rise over time. This acceleration is evident in the curves, where the progression becomes steeper following each delamination.

A notable observation in the adimensionalized curves is the apparent better fire resistance of WDCLT in relative terms. At a given charring progression rate and for the same number of charred layers, WDCLT demonstrates a higher relative residual capacity compared to glued CLT. While this may initially seem counterintuitive, it can be attributed to the connection system and the lower slip modulus of WDCLT. With reduced inter-layer collaboration, the effect of losing a layer in a composite beam with weakly collaborating layers is less pronounced than in a fully collaborating system. As a result, the adimensionalized resistance curves of WDCLT is superior to those of glued CLT. This highlights the influence of connection mechanics on fire resistance performance.

Table 9 summarizes the time values corresponding to specific load reduction factors (70%, 50%, 10%, and 1%) for panels with five, six, and seven layers, each 30 mm thick, comparing glued CLT and WDCLT. Compared to the fully glued configuration of CLT, the effect of weaker connections between layers in WDCLT is evident across all load ratios. As the number of layers increases from five to seven, the time to reach each load reduction factor increases for both typologies. This is expected since additional layers provide more material to resist thermal degradation and preserve load capacity. For the five-layer configuration, glued CLT reaches a 10% load ratio at 80 min and loses all load

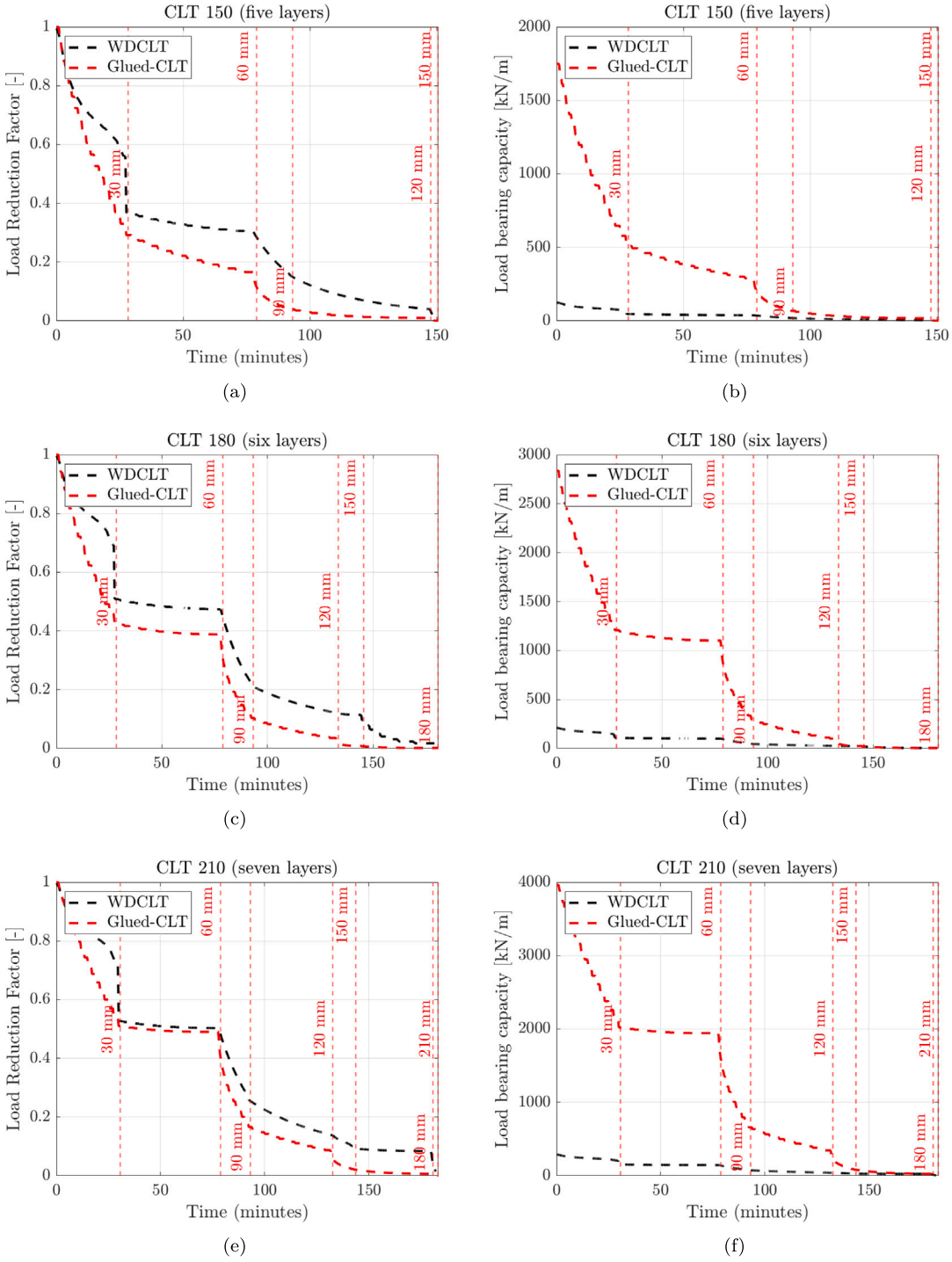

Fig. 15. Adimensional fire resistance of WDCLT walls with the delamination of the first two charred layers of (a)–(b) five, (c)–(d) six and (e)–(f) seven layers 30 mm thick. Each subplot shows the case of WDCLT vs. glued CLT.

capacity by 140 min. In contrast, WDCLT retains its load capacity for longer, reaching a 10% load ratio at 107 min and fully degrading at 149 min. This indicates that WDCLT offers approximately 10%–27% more resistance time than glued CLT for this configuration. For the six-layer configuration, the performance of glued CLT improves slightly, with a 10% load ratio reached at 94 min and collapse occurring at 148 min. However, WDCLT significantly outperforms glued CLT, with a 10% load ratio at 145 min and collapse at 179 min. This demonstrates a much more significant improvement in resistance for WDCLT as the number of layers increases, highlighting its better scalability with thickness. The trend continues in the seven-layer configuration, with glued CLT achieving a 10% load ratio at 123 min and collapsing at 159 min. WDCLT, however, achieves a 10% load ratio at 148 min and collapses at 182 min, further reinforcing its superior fire resistance as the number of layers increases.

The key observation is that WDCLT consistently delays the relative capacity loss compared to glued CLT. This is due to WDCLT's lower slip modulus, which reduces its sensitivity to fire-induced weakening. As a result, WDCLT maintains its original structural integrity for a longer duration under fire conditions. On average, when failure is defined as reaching 1% of the initial load, the time to failure is extended by approximately 50% in WDCLT compared to glued CLT.

Compared to the fully glued configuration of CLT, the effect of weaker interlayer connections in WDCLT results in lower overall stiffness. However, this lower slip modulus reduces the panel's sensitivity to fire-induced degradation. As layers progressively char and lose mechanical function, the relative capacity reduction in WDCLT is more gradual than in glued CLT, which relies heavily on composite action. This leads to a longer structural endurance under fire exposure, despite its lower initial capacity.

5. Conclusions

Adhesive-free cross-laminated timber (CLT) panels are gradually re-emerging in timber engineering research and specific niche markets, mainly due to their environmentally friendly advantages compared to adhesive-bonded CLT. The tested panels are connected using dried beech dowels. The dowels naturally swell as they reach the moisture content equilibrium with the surrounding panels and environment, ensuring the mechanical integrity of the system. However, the bending stiffness of adhesive-free CLT can be more than ten times lower than that of glued CLT, which represents a significant drawback in terms of mechanical performance.

In this study, the fire resistance of wooden dowelled CLT (WDCLT) was investigated. A large-scale fire test was conducted on an unprotected 3 m × 3 m WDCLT panel, placed vertically and exposed to fire on one side. The average charring rate was approximately 0.9 mm/min, slightly higher than that of glued CLT under similar testing conditions. The primary reason, as shown in this study, was the fall-off of the first two charred layers, which exposed uncharred wood during the fire test. This led to two phases of accelerated charring rates: one in the initial phase and another after the fall-off of the first two layers.

Additionally, the increased deformability of the WDCLT panel under load may increase the likelihood of charred layer detachment compared to glued CLT panels. As the charred layer, with almost zero capacity, cannot accommodate the increased deformations, this could potentially accelerate degradation. Therefore, the likelihood of delamination may be higher in WDCLT than glued, even when laid vertically. However, further testing is required to draw definitive conclusions. Notably, the 180 mm-thick, 6-layer WDCLT panel, with each layer 30 mm thick, successfully supported a load of 50 kN/m for 100 min.

Single burning tests were also conducted, which led to the classification of the WDCLT panel as D-s1, d0, with slightly lower smoke production compared to typical glued CLT, which is often classified as D-s2, d0.

A thermomechanical model was developed with two main objectives: indirectly estimating the evolution of charring depth from the panel's deformation history, as no temperature measurements within the panel thickness were available, and performing parametric analyses. These analyses aimed to estimate the load-bearing capacity ratio over time as a function of the WDCLT layup, compare glued versus dowelled CLT performance, and examine the impact of sudden charred layer fall-off on these panels.

The fall-off of the charred layers primarily impacts the final stages of the resistance curve, particularly the time required to reach 10% of the initial load-bearing capacity and complete failure. When comparing glued CLT to WDCLT, where the only difference lies in the connection between lamellae, fully collaborating in the former and with a slip modulus of 1.69 kN/mm in the latter, WDCLT exhibits superior performance in relative terms (ratio between time at a given time and the initial load bearing capacity). While this may initially seem counterintuitive, it can be explained by the connection system and the lower slip modulus of WDCLT. With reduced inter-layer collaboration, the effect of losing a layer in a composite beam with weakly collaborating layers is less pronounced than in a fully collaborating system. As a result, the adimensionalized resistance curves of WDCLT are superior to those of glued CLT.

This study is based on a single full-scale WDCLT specimen, and while it provides relevant information, the results should be interpreted with caution due to potential variability arising from factors such as moisture content, dowel density, and fabrication tolerances. Additionally, the fire performance was assessed in a vertical configuration; further investigations are necessary to evaluate the behaviour of WDCLT in horizontal applications, where the risk of delamination and gravity-induced separation is more critical. Future research should include sensitivity analyses, repeat tests, and comparative studies on different orientations to enhance the generalizability and robustness of the findings.

CRediT authorship contribution statement

Angelo Aloisio: Writing – review & editing, Writing – original draft, Visualization, Validation, Supervision, Software, Resources, Project administration, Methodology, Investigation, Funding acquisition, Formal analysis, Data curation, Conceptualization. **Dag Pasquale Pasca:** Writing – review & editing, Writing – original draft, Validation, Supervision, Methodology, Data curation, Conceptualization. **Massimo Fragiacomo:** Writing – review & editing, Validation, Methodology.

Declaration of competing interest

All authors have participated in (a) conception and design, or analysis and interpretation of the data; (b) drafting the article or revising it critically for important intellectual content; and (c) approval of the final version.

This manuscript has not been submitted to, nor is under review at, another journal or other publishing venue.

The authors have no affiliation with any organization with a direct or indirect financial interest in the subject matter discussed in the manuscript

Acknowledgements

The authors express their gratitude to the Italian company BIOHABITAT s.r.l. (Folgaria, Trento, Italy), which commissioned the fire tests on the WDCLT they produced, for sharing the data underlying this research.

This work was developed in the framework of the COST Action CA20139 – "Holistic design of taller timber buildings (HELEN)", and it is the outcome of the Short-Term Scientific Mission (STSM) Grant of the first author – Ref. E-COST-GRANT-CA20139-1d456e25.

Appendix. Estimation of the slip modulus from push-out tests

The value for the slip modulus was obtained from additional push-out tests, and the final bending stiffness was verified through three-point bending tests. The push-out test was carried out by the company BIOHABITAT; see Fig. A.16. When the panel bends, compression and tension forces act in opposite directions, resulting in a slip between the layers, as the dowelled connection is not perfectly rigid. To simulate the sliding between the top and bottom layers of the WDCLT panel, a 750 × 180 specimen consisting of a 6-layer WDCLT panel (layup 180 mm, see Fig. 2) has been tested.

The test procedure started with the failure of a pilot specimen to estimate the failure load (F_{est}) for the remaining ten specimens. A cyclic loading procedure followed, beginning with the application of a load equal to $0.5 \cdot F_{est}$, held for 30 s, and then unloading to $0.1 \cdot F_{est}$, held again for 30 s. The load was then reapplied until either the ultimate load was reached or a 15 mm slip occurred, whichever came first. Displacement measurements were recorded throughout the test. The testing machine applied the load at a constant rate, ensuring that either the ultimate force or the 15 mm slip was reached within 5 to 7 min.

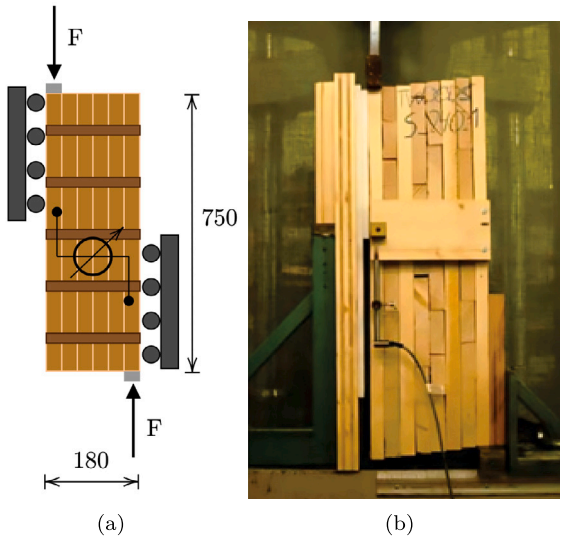

Fig. A.16. (a) Experimental setup of the push-out tests (b) View of the push-out specimens after the tests.

Table A.10
Results of the push-out tests and slip modulus estimation. F_{max} is the maximum force from push-out tests and $u_{0.1}$ and $u_{0.4}$ the displacements corresponding to 0.1 F_{max} and 0.4 F_{max}.

Sample No.	0.1 F_{max} [kN]	0.4 F_{max} [kN]	$u_{0.1}$ [mm]	$u_{0.4}$ [mm]	Slip modulus [kN/mm]
1	9.81	0.98	2.94	0.30	1.67
2	10.49	1.05	3.15	0.33	1.67
3	10.06	1.01	3.02	0.25	1.63
4	8.79	0.88	2.64	0.34	1.72
5	9.38	0.94	2.81	0.31	1.69
6	8.01	0.80	2.40	0.29	1.71
7	7.95	0.80	2.39	0.40	1.80
8	10.40	1.04	3.12	0.24	1.63
9	8.33	0.83	2.50	0.29	1.70
10	8.93	0.89	2.68	0.24	1.65
				Mean	1.62
				CoV	0.03

The slip modulus of the connection was calculated using Eq. (A.1) according to EN26891 [50].

$$K = \frac{0.4F_{est} - 0.1F_{est}}{u_{0.4} - u_{0.1}} \tag{A.1}$$

where F_{est} is the estimated load, u is the relative displacement corresponding to the applied load.

Table A.10 shows the results of the push-out tests, where the force values and slip modulus refer to a single connector.

Data availability

Data will be made available on request.

References

[1] of Italy Trees NRC, (Cnr-Ivalsa) TI. Scientific report, progetto sofie – sistema costruttivo fiemme. Tech. rep., Autonomous Province of Trento; 2007, in Italian.
[2] für Holzbau und Holztechnologie und Holz I. BSPhandbuch - holz-massivebauweise in brettsperrholz. Graz: Bau Forschungs GmbH; 2010.
[3] Gagnon S, Pirvu C. CLT handbook: cross-laminated timber. Special Publication SP-528E, Quebec: FPInnovations; 2011.
[4] Brandner R, Flatscher G, Ringhofer A, Schickhofer G, Thiel A. Cross laminated timber (clt): overview and development. Eur J Wood Wood Prod 2016;74(3):331–51. http://dx.doi.org/10.1007/s00107-015-0999-5.
[5] Sandoli A, D'Ambra C, Ceraldi C, Calderoni B, Prota A. Sustainable cross-laminated timber structures in a seismic area: Overview and future trends. Appl Sci 2021;11(5):1–24. http://dx.doi.org/10.3390/app11052078.
[6] Cadorel X, Crawford R. Life cycle analysis of cross laminated timber in buildings: a review (n.d.).
[7] Lim H, Tripathi S, Tang JD. Bonding performance of adhesive systems for cross-laminated timber treated with micronized copper azole type c (mca-c). Constr Build Mater 2020;232:117208. http://dx.doi.org/10.1016/j.conbuildmat.2019.117208.
[8] Zelinka SL, Sullivan K, Pei S, Ottum N, Bechle NJ, Rammer DR, et al. Small scale tests on the performance of adhesives used in cross laminated timber (clt) at elevated temperatures. Int J Adhes Adhes 2019;95. http://dx.doi.org/10.1016/j.ijadhadh.2019.102436.
[9] Sotayo A, Bradley DF, Bather M, Oudjene M, El-Houjeyri I, Guan Z. Development and structural behaviour of adhesive free laminated timber beams and cross laminated panels. Constr Build Mater 2020;259:119821. http://dx.doi.org/10.1016/j.conbuildmat.2020.119821.
[10] Han L, Kutnar A, Sandak J, Šušteršič I, Sandberg D. Adhesive-and metal-free assembly techniques for prefabricated multi-layer engineered wood products: A review on wooden connectors. Forests 2023;14(2):311. http://dx.doi.org/10.3390/f14020311.
[11] Nakos P, Achelonoudis C, Papadopoulou E, Athanassiadou E, Karagiannidis E. Environmentally-friendly adhesives for wood products used in construction applications. In: World conference on timber engineering. WCTE, 2016.
[12] Hussin MH, Abd Latif NH, Hamidon TS, Idris NI, Hashim R, Appaturi JN, et al. Latest advancements in high-performance bio-based wood adhesives: A critical review. J Mater Res Technol 2022;21:3909–46. http://dx.doi.org/10.1016/j.jmrt.2022.10.156.
[13] Eta-23/0041. lignoloc® wood-based dowel type fasteners. Tech. rep., 2023.
[14] Z-9.1-899. tragende holzverbindungen unter verwendung von lignoloc® holznägeln. Tech. rep., 2020.
[15] Giordano L, Derikvand M, Fink G. Bending properties and vibration characteristics of dowel-laminated timber panels made with short salvaged timber elements. Buildings 2023;13(1):99. http://dx.doi.org/10.3390/buildings13010199.
[16] O'Ceallaigh C, Harte AM, Mcgetrick PJ. Dowel laminated timber elements manufactured using compressed wood dowels. In: Civil engineering research in Ireland. CERI 2022, 2022, p. 222–7.
[17] Sotayo A, Bradley D, Bather M, Sareh P, Oudjene M, El-Houjeyri I, Harte AM, Mehra S, O'Ceallaigh C, Haller P, et al. Review of state of the art of dowel laminated timber members and densified wood materials as sustainable engineered wood products for construction and building applications. Dev Built Environ 2020;1:100004.
[18] Bocquet J-F, Pizzi A, Despres A, Mansouri HR, Resch L, Michel D, et al. Wood joints and laminated wood beams assembled by mechanically-welded wood dowels. J Adhes Sci Technol 2007;21(4):301–17. http://dx.doi.org/10.1163/156856107780684585.
[19] Biwôlé JJE, Biwolé AB, Pizzi A, Mfomo JZ, Segovia C, Ateba A, et al. A review of the advances made in improving the durability of welded wood against water in light of the results of african tropical woods welding. J Renew Mater 2023;11(3):1077–99. http://dx.doi.org/10.32604/jrm.2023.024079.
[20] O'Loinsigh C, Oudjene M, Ait-Aider H, Fanning P, Pizzi A, Shotton E, et al. Experimental study of timber-to-timber composite beam using welded-through wood dowels. Constr Build Mater 2012;36:245–50. http://dx.doi.org/10.1016/j.conbuildmat.2012.04.118.
[21] Grönquist P, Schnider T, Thoma A, Gramazio F, Kohler M, Burgert I, et al. Investigations on densified beech wood for application as a swelling dowel in timber joints. Holzforschung 2019;73(6):559–68. http://dx.doi.org/10.1515/hf-2018-0106.
[22] Pereira MCdM, Pascal Sohier LA, Descamps T, Junior CC. Doweled cross laminated timber: Experimental and analytical study. Constr Build Mater 2021;273:121820. http://dx.doi.org/10.1016/j.conbuildmat.2020.121820.
[23] Frangi A, Fontana M, Hugi E, Jöbstl R. Experimental analysis of cross laminated timber panels in fire. Fire Saf J 2009;44(8):1078–87.
[24] Frangi A, Fontana M, Knobloch M, Bochicchio G. Fire behaviour of cross-laminated solid timber panels. Fire Saf Sci 2009;9:1279–90.
[25] Wilinder P. Fire resistance in cross-laminated timber. 2010.
[26] Friquin K, Grimsbu M, Hovde P. Charring rates for cross-laminated timber panels exposed to standard and parametric fires. In: Proc world conference on timber engineering. Riva del Garda; 2010.
[27] Teibinger M, Matzinger I. Basis for evaluation of the fire resistance of timber constructions. Tech. rep., Vienna: Holzforschung Austria; 2010.
[28] Osborne L, Dagenais C, Bénichou N. Preliminary clt fire resistance testing report. Tech. rep., Ottawa: FPInnovations NRC CNRC; 2012.
[29] Fragiacomo M, Menis A, Clemente I, Bochicchio G, Ceccotti A. Fire resistance of cross-laminated timber panels loaded out-of-plane. J Struct Eng 2013;139(12):04013018. http://dx.doi.org/10.1061/(ASCE)ST.1943-541X.0000787.
[30] Fragiacomo M, Menis A, Clemente I, Bochicchio G, Ceccotti A. Fire resistance of cross-laminated timber panels loaded out of plane. J Struct Eng 2013;139(12):04013018.

[31] Frangi A, Bochicchio G, Ceccotti A, Lauriola P. Natural full-scale fire test on a 3 storey xlam timber building. In: Proc world conference on timber engineering. Miyazaki; 2008.
[32] Klippel M, Leyder C, Frangi A, Fontana M, Lam F, Ceccotti A. Fire tests on loaded cross-laminated timber wall and floor elements. In: Proc international symposium on fire safety science. Christchurch: University of Canterbury; 2014.
[33] Klippel M, Schmid J. Design of cross-laminated timber in fire. Struct Eng Int 2017;27(2):224–30. http://dx.doi.org/10.2749/101686617X14881932436096.
[34] Schmid J, König J, Köhler J. Fire exposed cross-laminated timber – modelling and tests. In: Proc CIB-w18 meeting. Nelson; 2010.
[35] Jabar KA, Husain H, Smith W, Lee LSH. Fire performance of endospermum malaccense cross laminated timber (clt) treated with fire retardant. Environ-Behav Proc J 2024;9(SI17):3–9.
[36] Zheng X, He M, Li Z, Lou G, Li G-Q. Experimental investigation into the effect of transparent fireproof coatings on charring behavior of glued laminated timber exposed to fire. Fire Saf J 2024;104274.
[37] Din en 1363-1: Fire resistance tests - part 1: General requirements. 2020.
[38] Liu J, Fischer EC. Review of the charring rates of different timber species. Fire Mater 2024;48(1):3–15.
[39] Klippel M, Leyder C, Frangi A, Fontana M, Lam F, Ceccotti A. Fire tests on loaded cross-laminated timber wall and floor elements. Fire Saf Sci 2014;11(2014):626–39.
[40] Klippel M, Schmid J, Frangi A. Fire design of clt. In: Proceedings of the joint conference of COST actions FP1402 & FP1404 KTH building materials, cross laminated timber—a competitive wood product for visionary and fire safe buildings. 2016, p. 101–22.
[41] Commission decision of 8 february 2000 implementing council directive 89/106/eec as regards the classification of the reaction to fire performance of construction products. 2000, https://eur-lex.europa.eu/legal-content/EN/TXT/?uri=CELEX%3A32000D0147.
[42] Östman BA-L, Mikkola E. European classes for the reaction to fire performance of wood-based panels. Fire Mater 2010;34(6):315–30.
[43] EN 13238: Reaction to fire tests for building products—Conditioning procedures and general rules for selection of substrates. 2001.
[44] Liu J, Fischer EC. Review of large-scale clt compartment fire tests. Constr Build Mater 2022;318:126099.
[45] Janssens M, Albracht N, Carpenter K. Full-scale tests in a furnished living room to evaluate the fire performance of protected cross-laminated and nail laminated timber construction. Southwest Research Institute; 2015.
[46] for Standardization EC. EN 1991-1-2: eurocode 1-actions on structures - part 1-2: general actions – actions on structures exposed to fire. Brussels: European Committee for Standardization; 2002.
[47] for Standardization IO. ISO 834–1: fire resistance tests. elements of building construction. part 1: general requirements. Geneva: ISO; 1999.
[48] European Commission. A new circular economy action plan. 2020.
[49] Ballio G, Mazzolani FM. Theory and design of steel structures. Taylor & Francis; 1983.
[50] CEN. En 1995 eurocode 5: Design of timber structures. 2004.
[51] Kreuzinger H. Mechanically jointed members and clt elements. 2017, p. 249–62, Ch. 7.
[52] Blaß HJ, Sandhaas C. Timber engineering-principles for design. KIT scientific publishing; 2017.
[53] Breyer DE. Design of wood structures. 1988.
[54] Amin R, Mo Y, Richter F, Kurzer C, Werther N, Rein G. Predicting the average charring rate of mass timber using data-driven methods for structural calculations. Fire Technol 2024;60(6):4001–21.
[55] Van der Westhuyzen S, Walls R, De Koker N. Fire tests of south african cross-laminated timber wall panels: fire ratings, charring rates, and delamination. J South Afr Inst Civ Eng 2020;62(1):33–41.
[56] Pečenko R, Knez N, Hozjan T, Šejna J, Cabová K, Turk G. On the char front temperature of beech (fagus sylvatica). Wood Sci Technol 2024;58(4):1535–53.
[57] Fragiacomo M, Menis A, Moss P, Buchanan A, Clemente I. Numerical and experimental evaluation of the temperature distribution within laminated veneer lumber (lvl) exposed to fire. J Struct Fire Eng 2010;1(3):145–59.
[58] Fragiacomo M, Menis A, Moss P, Clemente I, Buchanan A, Nicolo BD. Predicting the fire resistance of timber members loaded in tension. Fire Mater 2013;37(2):114–29. http://dx.doi.org/10.1002/fam.2117.
[59] Klippel M, Frangi A, Fontana M. Influence of the adhesive on the load-carrying capacity of glued laminated timber members in fire. In: Proc symposium on fire safety science. Baltimore: University of Maryland; 2011.
[60] for Standardization (CEN) EC. EN 1995-1-2: eurocode 5-design of timber structures. part 1-2: general - structural fire design. Brussels: European Committee for Standardization; 2004.
[61] Schmid J, Menis A, Fragiacomo M, Bostrom L, Just A, Gustafsson eaA. The load bearing performance of clt wall elements in large-scale fire tests. In: Proc. international fire science and engineering conference INTERFLAM. London: University of London; 2013.